Published in final edited form as:
J Neurosci. 2008 December 24; 28(52): 14074–14086. doi:10.1523/JNEUROSCI.3188-08.2008.

Id2 IS REQUIRED FOR SPECIFICATION OF DOPAMINERGIC NEURONS DURING ADULT OLFACTORY NEUROGENESIS

Matthew C. Havrda[1], **Brent T. Harris**[2], **Akio Mantani**[3], **Nora M. Ward**[1], **Brenton R. Paolella**[1], **Verginia C. Cuzon**[4], **Hermes H. Yeh**[4], and **Mark A. Israel**[1]

1*Norris Cotton Cancer Center, Department of Genetics, Dartmouth Medical School, Lebanon NH*

2*Department of Pathology, Dartmouth Hitchcock Medical Center, Lebanon, NH*

3*Division of Psychiatry, Yoshida General Hospital, Hiroshima, Japan*

4*Department of Physiology, Dartmouth Medical School, Lebanon, NH*

Abstract

Understanding the biology of adult neural stem cells has important implications for nervous system development and may contribute to our understanding of neurodegenerative disorders and their treatment. We have characterized the process of olfactory neurogenesis in adult mice lacking Inhibitor of DNA Binding 2 (*Id2*). We found a diminished olfactory bulb containing reduced numbers of granular and periglomerular neurons with a distinct paucity of dopaminergic periglomerular neurons. While no deficiency of the stem cell compartment was detectable, migrating neuroblasts in $Id2^{-/-}$ mutant mice prematurely undergo astroglial differentiation within a disorganized rostral migratory stream. Further, when evaluated *in vitro* loss of *Id2* results in decreased proliferation of neural progenitors and decreased expression of the Hes1 and Mash1 transcription factors, known mediators of neuronal differentiation. These data support a novel role for sustained *Id2* expression in migrating neural progenitors mediating olfactory dopaminergic neuronal differentiation in adult animals.

Keywords

Id2; dopaminergic; olfactory; adult; neurogenesis; subventricular zone

INTRODUCTION

A subset of olfactory bulb (OB) neurons in adult mice undergo apoptotic death and are replaced by ongoing neurogenesis (L. Petreanu and A. Alvarez-Buylla, 2002). Stem cells responsible for replacement of olfactory neurons reside in the subventricular zone (SVZ), a cell compartment lining the anterior lateral ventricles (C. Lois et al., 1996; F. Doetsch et al., 1997; J. M. Garcia-Verdugo et al., 1998; L. Petreanu and A. Alvarez-Buylla, 2002). Studies of neuronal progenitors residing in the SVZ indicate three distinguishable cell types. These include PSA-NCAM or Doublecortin (Dcx) expressing migrating neuroblasts (type-A cells), proliferative GFAP expressing cells (type-B cells), and transient amplifying precursor cells (type-C cells) (M. H. Porteus et al., 1994; K. Yun et al., 2001; J. Stenman et al., 2003; M. Kohwi et al., 2005).

Corresponding Author: Matthew C. Havrda Ph.D., Norris Cotton Cancer Center, Dartmouth Medical School, 1 Medical Center Drive, Rubin 7, Rm. 751, Lebanon, NH 03756, E-mail: Matthew.C.Havrda@Dartmouth.edu.

The adult SVZ is the sole source of adult born olfactory neurons (M. Lemasson et al., 2005). The granular cell layer (GCL) and periglomerular cell layer (PGL) interneurons replaced in the OB are diverse in their neurotransmitter profile (G. M. Shepherd et al., 2007). Two distinct olfactory interneurons make up the majority of those arising in adults: GABAergic, calretinin (CR) expressing neurons, and dopaminergic tyrosine hydroxylase (TH) expressing neurons (S. De Marchis et al., 2007). *Small eye* mice carry a mutation in the *Pax6* gene and the eyes and olfactory system of these animals fail to develop. Studies of mice hemizygous for *Pax6* reveal a depletion of OB dopaminergic neurons (A. Stoykova and P. Gruss, 1994; T. L. Dellovade et al., 1998; M. Kohwi et al., 2005).

During neurogenesis highly conserved pro-neural basic helix-loop-helix (bHLH) transcription factor dimers mediate differentiation (F. Guillemot, 1999; N. Bertrand et al., 2002; J. H. Chae et al., 2004). These include Mash1 and genes of the *Neurogenin* (*Ngn*) and *NeuroD* families (F. Guillemot, 1999). High levels of neuro-inhibitory *Hes1* are expressed in the SVZ and RMS allowing stem and progenitor cells to proliferate en route to the OB where *Hes1* expression diminishes and neuronal differentiation occurs (T. Ohtsuka et al., 2006).

Members of the *Id* gene family inhibit the activity of bHLH transcription factors by blocking their dimerization with bHLH proteins (R. Benezra et al., 1990; A. Jogi et al., 2002). Most commonly this results in the inhibition of differentiation (L. Cai et al., 2000) and promotion of proliferation (A. Iavarone et al., 1994). Id expression is very limited in adult tissues but is detectable in distinct populations of adult post-mitotic neurons including the GCL and PGL of the OB and striatal dopaminergic cells including the caudate-putamen and substantia nigra (SN) (K. Kitajima et al., 2006). We observed that the brains of $Id2^{-/-}$ mice appear to develop normally although the OB of adults is significantly smaller than it is in WT littermates. While *Id2* appears dispensable for adult SVZ function, neuronal precursors have an altered differentiation potential resulting in decreased OB dopaminergic neurons. Finally, we demonstrate that loss of Id2 inhibition of Hes1 results in decreased *Mash1* expression, a known requirement for dopaminergic neuronal differentiation.

MATERIALS AND METHODS

Targeted Deletion of Id2

Homologous recombination-based gene targeting in ES cells was employed to inactivate the *Id2* locus in the murine C57BL/6 strain. The *Id2* targeting vector contained the neomycin phosphotransferase resistance gene driven by the thymidine kinase promoter located immediately 5’ from the third exon of the endogenous *Id2* gene. Homologous recombination was verified in resistant clones using Southern blot analysis with presence of the mutant allele resulting in a 3kb reduction in size of the *Id2* locus as the result of replacement of exons 1 and 2 of the *Id2* locus by the targeting cassette. C57BL/6 mice were then outbred into a CD1 background to produce a mixed strain and maintained on a diet containing an antibiotic (Septra, Harlan) and breeding was enhanced with a high fat reproductive supplement (Love-Mash, Bio-Serv). Genotyping of mice was conducted with the following primers: CAA AAC TGT AGC CCT CTG AG, AGG CGC CAG TCT GCT TCT TGT AAC, TAG CCT GAA GAA CGA GAT CAG CAG, which identify both the WT and mutant allele, with hemizygous mice generating both bands.

Tissue Harvest, Sectioning, and Cell Quantitation

Brains were perfusion-fixed and dissected followed by either paraffin embedding or preparation for cryosectioning by sucrose protection and embedding in OCT media. Serial histological sections were obtained from $Id2^{-/-}$ and WT littermate controls or age-matched non-littermate controls as indicated in the text. For evaluation of OB laminar structure, paraffin

sections were stained with hematoxylin and eosin. For area measurements, multiple serial sections from *Id2*$^{-/-}$ and WT littermate controls were aligned and analyzed. Digital images were obtained using a compound microscope and digital camera (Olympus), and the area of each aligned section was quantified using image analysis software (Imagepro 5.1).

To determine the concentration of immunostained cells within the GCL and PGL, we first identified corresponding histological sections from *Id2*$^{-/-}$ and WT mice at three rostrocaudal levels evenly spaced at ~100 μm intervals beginning at the most rostral section in which the accessory OB was not visible. We counted immunostained cells per unit area in corresponding sections on the medial side of the OB using a defined 100μM^2 grid generated by image analysis software. No fewer than eight sections for each of six animals per genotype were analyzed. Statistical significance was determined using a two–tailed Students-T-test with a threshold p-value of 0.05.

Anosmia Analysis

A buried food paradigm was used as described (J. W. Harding et al., 1978). A single pellet of a high fat food supplement used to rear *Id2*−/− mice (Love Mash Reproductive Diet, Bioserve) was buried in a corner 3 cm below the surface of bedding in a clean cage. The mice were fasted for 16 hours before a set of trials. For each trial the mouse was placed in the center of the cage and given a maximum of five minutes to find the pellet of food. Mice were considered to have found the food once they excavated and made physical contact with the food pellet. To ensure that memory did not play a role in the test, the pellets for the second and third trials were buried in different corners of the cage at 5 cm and 1 cm depth respectively. For the fourth trial the food was buried in the center of the cage at a depth of 3 cm. If the food had not been found at the end of five minutes, the trial was terminated. Data were analyzed for significance using the Student's t-test.

Olfactory Discrimination

Olfactory discrimination analysis was performed as previously described (G. Gheusi et al., 2000). Briefly, 15μl of vanilla scented essential oil diluted 1:10,000 in water was put on filter paper and placed at one end on the floor of the animal's home cage. An identical filter paper with 15ml of sterilized water was placed on the opposite end of the cage as a control. A habituation-dishabituation task was performed in which vanilla was presented for five successive trials of 3 min each separated by 15 min intervals. On the sixth trial, the mouse was exposed for 3 min to diluted orange scented oil just as in the vanilla trials. Mice were considered to be investigating the odor whenever their noses were 1 cm or less from the filter paper. Data were analyzed for significance using the Mann-Whitney-Wilcoxon rank-sum test.

Immunohistochemistry

Immunochemistry was performed on either paraffin embedded or cryopreserved sections as required by specific antibodies. All paraffin embedded sections were analyzed following antigen retrieval using 0.1M citrate buffer unless otherwise specified. Mature olfactory granule and periglomerular neurons were identified using anti-NeuN (Chemicon) antibody. Adult born neuronal sub-types were labeled using anti-calretinin (CR) (Novus) and anti-tyrosine hydroxylase (TH) (Chemicon) antibodies. Astroglial lineages were stained using anti-GFAP (Dako) antibody and oligodendroglial lineages were identified by reactivity to anti-Olig2 or anti-O4 (Chemicon) antibodies. Biotinylated secondary antibodies include anti-mouse and rabbit (Vector Laboratories) antibodies. For fluorescent labeling of frozen sections antigen retrieval was performed using 0.2% Triton in PBS. For immunoflourescence, neuroglial subtypes were identified with anti-Tuj1 (Promega) antibodies and antibodies that recognize NeuN, GFAP, CR, and TH as described above. Migrating neuroblasts were labeled with anti-doublecortin (Dcx) (Abcam) antibody. Fluorescent secondary antibodies include mouse and

rabbit 555 and 488 (Alexaflour). Paraffin sections were counterstained with hematoxylin and fluorescent stains with Hoechst Dye (Sigma).

5-bromo-2′-deoxyuridine Treatment, and Neural Progenitor Cell Analysis in the Subventricular Zone, and Rostral Migratory Stream

Cell quantification of neural progenitor cells in the SVZ and newborn neuroblasts in the RMS were evaluated by differential BRDU retention as previously described (C. M. Morshead and D. van der Kooy, 1992; C. M. Morshead et al., 1998). To identify SVZ born migrating neuroblasts, WT and *Id2*$^{-/-}$ mice were injected intraperitoneally with BRDU (80mg/kg) twice daily for 4 days and sacrificed on day 6. Cells were quantified from saggital sections in three locations including the vertical, horizontal, and elbow sections on the RMS as previously described by Martoncikova et al. (M. Martoncikova et al., 2006) and expressed as total number of positive cells in each section compared to WT controls. To interrogate only SVZ stem cells (type-B cells) (F. Doetsch et al., 1999), mice were injected as above twice daily for 12 days and left for an additional 16 days prior to sacrifice and histological preparation. Sequential saggital sections were co-stained for GFAP (Dako) and BrdU (Novus). Type-B cells were identified as BRDU/GFAP double-positive as opposed to GFAP+/BRDU-astrocytes.

Proliferation and Apoptosis Analysis

Neural precursor cells were explanted from the brains of post-natal mice between 1 and 3 days of age and propagated as described (B. A. Reynolds and S. Weiss, 1992, 1996). For the evaluation of cell growth, 20,000 cells/well were plated in ultra-low binding 24 well plates (Corning). Cell numbers were quantified using a hemacytometer at 2, 4, 6, and 8 days following plating from three separate wells. To determine the cell cycle distribution of WT and *Id2*$^{-/-}$ cells, primary neurospheres were dissociated and stained with propidium iodide (PI), and quantified using cell cycle analysis software (Modfit). For *in vitro* BrdU incorporation cells were plated 24 hours prior to the addition of 1mg/ml BRDU directly into proliferation media. At specific time points cells were dispersed and BRDU labeling was conducted following pre-treatment with 2N HCL using a FITC-conjugated BRDU primary antibody (eBiosciences) followed by detection using flow cytometry. To measure sphere size cells plated in 10cm Petri dishes were photographed at indicated time points and sphere area was measured using image analysis software (ImagePro). To evaluate apoptosis in sphere cultures, trypsinized single cell suspensions were stained using the 7-Amino-actinomycin D and Annexin-V Kit per manufacturer's recommendations (Guava-Nexin, Guava Technologies). Analysis of apoptosis in adherent differentiating cells were quantified by examination of chromatin condensation by Hoechst 33342 staining (Sigma) combined with chromatin fragmentation identified by terminal deoxynucleotidyltransferase-mediated dUTP nick end-labeling (TUNEL) (Roche) as previously described (P. J. Andres-Barquin et al., 1999). T-test analysis was performed as above.

Luciferase Assays

Cultured neurospheres were co-transfected using adenovirus-assisted transfection for increased efficiency. Empty adenoviral vectors or *Id2* adenovirus, constitutively activated Notch1 (NICD1) (generously provided by Dr. Lucy Liaw, Maine Medical Center Research Institute), Hes1-reporter and renilla normalization plasmids were co-transfected into 1e^{6} dispersed neural stem cells using Fugene (Roche). Cells were allowed to proliferate for 48 hours following transfection, harvested, and luciferase production determined and normalized to renilla (Dual-Luciferase Assay, Promega).

Real-Time PCR

Total RNA was collected from WT or *Id2*$^{-/-}$ neurospheres growing in proliferation conditions pre-treated with DNAase1 (Promega) and reverse transcribed using iScript reverse transcription mix (Bio-Rad). Samples incubated without reverse transcriptase were included as negative controls. Resultant cDNA was evaluated by quantitative RT-PCR (QT-PCR) for detection of *Hes1* transcript (primers available on request) using the iCycler thermocycler (Bio-Rad). PCR products were detected by incorporation of SYBR green (Bio-Rad) and authenticated by melt-curve and gel electrophoresis. Threshold cycle numbers during the log-phase of amplification were normalized to the expression of β-actin and Cyclophilin.

Western Blotting

Neurosphere lysates were collected and triturated into chilled lysis buffer [(150mM NaCl, 50mM Tris (pH8.0), 1% Triton X-100)] supplemented with 2.5% protease inhibitor cocktail (Sigma). Protein was quantified using a modified Bradford assay (Bio-Rad) and 60μg of total protein pre-cleared of insoluble material by centrifugation was analyzed on 15% acrylamide gels. Blots were probed with anti-*Id2* (Santa Cruz), ant1-*Hes1* (Chemicon), or anti-*Mash1* (Chemicon) antibodies. Protein loading will be controlled by normalization to β-actin (Sigma).

Chromatin Immunoprecipitation

Input material for chromatin immunoprecipitation assays included total genomic DNA from WT and *Id2*$^{-/-}$ cultured neurospheres in proliferation medium collected during steady state log-phase growth 48 hours following dispersion. Following cross-linking in 1% formaldehyde for 15 minutes, cells were collected, and genomic DNA was sheared to an average size of 500 base pairs using a sonicator. Immunoprecipitation was performed with 5μg of a polyclonal anti-Hes1 antibody (Chemicon) overnight. Cross-links were reversed at 65dg.C for 4 hours and DNA was collected by phenol-chloroform extraction and ethanol precipitation. PCR analysis was conducted using primers designed to frame multiple E-Boxes known to mediate *Hes1* auto-inhibition (K. Takebayashi et al., 1994; H. Hirata et al., 2002). Primer sequences specific to the murine *Hes1* promoter are 5'-TTGATTGACGTTGTAGCCTCCGGT (sense), 5'-GGCTCGTGTGAAACTTCCCAAACT (anti-sense) resulting in the amplification of a 175 bp product. Primer sequences specific to the *Mash1* promoter are 5' TGGTCAGGCCATCACGACATTGTA (sense), 5' TCCTTGGCTTCTGCTTTGGTTCCT (anti-sense) resulting in the generation of a 225 bp product.

RESULTS

Diminished Olfactory Bulb Size in *Id2*$^{-/-}$ Mice

Our laboratory has studied the role of *Id* genes in CNS development (K. Yun et al., 2004). While *Id2*$^{-/-}$ mice have no obvious developmental phenotype, we, and others observed defects in lactation and hematopoiesis that are easily detectable in adult animals [unpublished data, (Y. Yokota et al., 1999; S. Mori et al., 2000)]. Upon analysis of the brains of adult *Id2*$^{-/-}$ mice, we noted an obvious reduction in the size of the OB of *Id2*$^{-/-}$ adult mice compared to wild-type (WT) littermates (Figure 1A, B) (Y. Yokota, 2001). We quantitated the area of multiple morphometrically aligned histological sections at specific rostro-caudal locations (described in Experimental Procedures) to evaluate this apparent difference and observed that *Id2*$^{-/-}$ mice have a significant reduction in the size of the OB as measured in coronal sections (Supplementary Figure 1A). These mice, however, do not have a significant change in overall brain mass relative to total body mass (Supplementary Figure 1B).

The adult OB is a highly ordered structure with a discrete laminar organization of individual neuronal cell types. The afferent nerve fibers emanating from olfactory receptor neurons

converge on multiple glomeruli and synapse with dendrites from second order tufted and mitral cells whose axons project directly to the pyriform area of the olfactory cortex [for review, (G. M. G. Shepherd, C.A., 1998)]. Adult born granular neurons in the PGL and GCL modulate the activity of this afferent pathway (K. Mori and G. M. Shepherd, 1994; G. M. Shepherd et al., 2007). We undertook a histological analysis of the OB in WT and *Id2*$^{-/-}$ mice to characterize the cellular architecture of these structures. Sections stained with hematoxylin and eosin revealed that the OB of *Id2*$^{-/-}$ mice retained most of the typical laminar structure of the OB but had an internal plexiform layer (IPL) that was reduced in size and disorganized (Figure 1C, D).

Neuronal fibers of the IPL, which is its defining histological characteristic, are thought to represent both dendrodendritic arborizations of granular neurons projecting onto mitral cells and concentric afferent fibers from both tufted and mitral cells (K. Mori and G. M. Shepherd, 1994). We used intermediate neurofilament immunohistochemistry to highlight the IPL in WT and *Id2*$^{-/-}$ mice and found an extensive loss of fibers within the IPL of *Id2*$^{-/-}$ mice (Figure 1E, F). Granular neurons, mitral cells, and tufted cells are thought to project fibers into the IPL (G. M. G. Shepherd, C.A., 1998). We found that *Id2*$^{-/-}$ mice had normal numbers of mitral and tufted cells (data not shown), and therefore we interpret these findings to suggest that the reduced overall size of the OB most likely results from a loss of granular interneurons.

Ongoing neurogenesis in the adult replenishes granular interneurons of the GCL and PGL of the OB. Throughout life the OB is characterized by the production of newborn granular interneurons emanating from the SVZ and ongoing apoptosis of post-mitotic OB interneurons. Neural progenitor cells persist in the adult SVZ and give rise to neuroblasts that migrate to the OB and differentiate into mature GCL and PGL interneurons. To further characterize the reduced size of the OB in *Id2*$^{-/-}$ mice, we estimated the numbers of mature interneurons, astroglia, and oligodendroglia in the adult OB. We used immunohistochemical detection of NeuN to identify interneurons of the GCL (Figure 2A, B) and PGL (Figure 2D, E), GFAP to identify astroglia (Supplementary Figure 2A, C), and Olig2 to identify oligodendroglia (Supplementary Figure 2B, C) in the OB of WT and *Id2*$^{-/-}$ mice. We found a significant reduction in the concentration of NeuN positive cells in the GCL of *Id2*$^{-/-}$ mice as compared to the GCL of WT mice (Figure 2A, B), and an even greater reduction was noted in the PGL of *Id2*$^{-/-}$ mice (Figure 2C, D). Interestingly, we also detected an increased percentage of astroglia within the GCL of *Id2*$^{-/-}$ animals (Supplementary Figure 2A, C), although Olig2 staining did not reveal a significant difference in the representation of oligodendroglia (Supplementary Figure 2B, C).

Loss of *Id2* Results in a Specific Depletion of PGL Dopaminergic Neurons

Recent evidence has indicated that as many as 21 neurochemically distinct sub-types of interneurons exist within the adult OB (S. Parrish-Aungst et al., 2007). To further define the role of *Id2* in the biology of adult-born OB neurons within both the GCL and PGL, we evaluated two distinct cell populations in these layers which are highly dependent on adult neurogenesis (M. Lemasson et al., 2005; S. De Marchis et al., 2007). GABAergic inhibitory granule cells within both the GCL and PGL can be identified by expression of the calcium binding protein, calretinin (CR). The second adult born neurons residing within the PGL are dopaminergic and can be identified by the expression of tyrosine hydroxylase (TH), the rate limiting enzyme in the synthesis of dopamine [for review, (S. Bovetti et al., 2007)]. We used the expression of CR and TH to identify these different cell types for quantitation. Immunohistochemical analysis revealed a 40% depletion of TH positive neurons in the PGL accompanied by an observable reduction in TH positive neuropil (Figure 2E, F, I). This occurs in the absence of significant difference in the numbers of CR positive neurons in the GCL and the PGL of WT and *Id2*$^{-/-}$ mice (Figure 2G, H, I). We detected only very rare TH positive neurons within the GCL of

WT or *Id2*$^{-/-}$ mice (data not shown). These data indicate that *Id2* is important for maintenance of a normal population of dopaminergic OB PGL neurons and is not required to maintain normal levels of the CR positive non-dopaminergic neuronal sub-types.

Altered Olfaction in *Id2*$^{-/-}$ Mice

We tested olfactory sensitivity and discrimination in *Id2*$^{-/-}$ mice seeking to identify a physiological impact of *Id2* loss. Using a hidden reward challenge, we examined olfactory sensitivity and found that it was not different in WT and *Id2*$^{-/-}$ mice (data not shown) (V. A. Galton et al., 2007). To examine olfactory discrimination we used a habituation-dishabituation paradigm (G. Gheusi et al., 2000). In this model WT mice performed as expected with their initial interest in a primary odorant evidenced by the increased time spent examining the odorant during trials 1, 2, 3 (Figure 3) decreasing over time (trials 3, 4, 5; Figure 3) as mice habituated to the stimulus (Figure 3). Introduction of a different odorant following habituation resulted in the anticipated result of “dishabituation” in WT mice. This is reflected in the comparison of time spent investigating the new odorant (Figure 3, trial 6) as compared to the time spent investigating the primary odorant at the end of the habituation study (Figure 3, trial 5). We found that *Id2*$^{-/-}$ mice failed to habituate to the primary stimulus (Figure 3, trials 1–5) and showed no demonstratable dishabituation after the introduction of the novel odorant (Figure 3, trials 5, 6). These data, in combination with our histologic findings, indicate that *Id2*$^{-/-}$ mice have an intact primary sensory apparatus; however, they are defective in olfactory memory and discrimination. These functional characteristics are consistent with the proposed function of sensory modulation for granular cells of the OB (G. M. Shepherd et al., 2007).

Loss of *Id2* Does Not Affect Cell Survival *in vivo*

The decreased numbers of dopaminergic granular neurons in the OB (Figure 2) and the olfactory deficit that these animals exhibited (Figure 3) provide strong evidence of a role for *Id2* in the maintenance of cellular homeostasis, since these neurons are known to die throughout life and require replacement by ongoing neurogenesis (L. Petreanu and A. Alvarez-Buylla, 2002). Previous studies conducted in our laboratory have demonstrated a role for Id proteins in mediating apoptosis (M. Florio et al., 1998;P. J. Andres-Barquin et al., 1999). We sought therefore to characterize neuronal OB cell death in the GCL and PGL of adult *Id2*$^{-/-}$ mice (Supplementary Figure 3 A–D). For this analysis we used the TUNEL assay to examine serial histological sections of OB from WT and *Id2*$^{-/-}$ mice for evidence of apoptosis. We found no difference in the number of apoptotic nuclei in the GCL (Supplemental Figure 3A, B, E) and PGL (Supplemental Figure 3C, D, E) of WT and *Id2*$^{-/-}$ mice. In fact, quantitation in serial sections, suggested a slight decrease in the number of apoptotic cells in these OB regions of *Id2*$^{-/-}$ mice consistent with the role of *Id2* as a pro-apoptotic gene (Supplemental Figure 3E) (Florio et al., 1998). We sought to characterize cell death in the RMS in order to determine the level of apoptosis in migrating neuroblasts. As expected we observed TUNEL positive cells in histologic sections of the OB from both WT and *Id2*$^{-/-}$ mice (Supplemental Figure 3F, H), however, we found no evidence of apoptosis within the RMS in these same histologic sections (Supplemental Figure 3G, I). These data indicate that the loss of *Id2* does not affect the size of the adult OB by enhancing cell death *in vivo*.

Altered Olfactory Neurogenesis in Adult *Id2*$^{-/-}$ Mice

We sought to examine further olfactory neurogenesis in adult *Id2*$^{-/-}$ animals. Neuronal precursor type-C cells in the SVZ can be differentiated from long-term repopulating B-cells based on their cell cycle times (C. M. Morshead and D. van der Kooy, 1992; C. M. Morshead et al., 1998). To identify these cells, we inoculated mice for 7 consecutive days with BRDU and used immunohistochemical analysis to identify BRDU-positive, rapidly dividing, type-C cells within the SVZ, RMS, and into the OB. Type-B cells within the SVZ can be identified

based on long-term BRDU retention identified by immunohistochemical analysis 16-days following this same 7 day inoculation protocol (T. D. Merson et al., 2006). We were not able to detect differences in the numbers of type-C cells in the SVZ (Figure 4A–C). Double labeling with GFAP and long-term BRDU incorporation was used to detect type-B cells in the SVZ (data not shown), which are widely thought to be the most primitive neural stem cells (F. Doetsch et al., 1999). In this case, while rare double-positive cells were detectable in both WT and *Id2*$^{-/-}$ mice, they appeared in similar numbers and no change in the population of long-term repopulating cells in *Id2*$^{-/-}$ mice could be identified (data not shown). We interpret these findings to indicate that the germinal SVZ compartment containing type-B cells and their progeny was intact in *Id2*$^{-/-}$ animals and that a decrease in the numbers of type-B cells is not responsible for the OB phenotype we observed.

We observed that while BRDU labeled cells reach the OB through an intact RMS in *Id2*$^{-/-}$ mice, an easily and invariably observed alteration in the architecture of the RMS was detectable. Compared to WT littermates the RMS of *Id2*$^{-/-}$ mice was characterized by decreased RMS diameter (Figure 4D, E and data not shown), and the appearance of rogue GFAP/BRDU double positive cells located proximal to, but outside of the RMS proper (Figure 4E, arrows). To further evaluate the characteristics of migrating type-A cells in the RMS, we employed immunofluorescence to detect doublecortin (Dcx) (data not shown), which specifically labels migrating neuroblasts (H. K. Yang et al., 2004). As expected, in WT animals Dcx labeling reveals elongated cells in an organized migration pattern within the RMS tangential to the SVZ en route to the OB. In *Id2*$^{-/-}$ animals Dcx staining was much less intense and elongated cells were absent suggesting a loss of both cellular orientation and RMS organization. Also we did not identify the accumulation of BRDU-labeled neuroblasts within the RMS (Figure 4D, E). These findings indicate that while the SVZ produces normal numbers of type-C neuroblasts (Figure 4A–C), and apparent alteration in migrating type-A cells occurs resulting in a reduced diameter of the RMS and a loss of the characteristic histological appearance of the RMS.

These observations of an altered RMS and our previous data suggesting that increased numbers of astroglia are present in the OB (Supplementary Figure 1A) led us to more critically examine the possibility that *Id2* loss led to increased numbers of astroglia within the OB at the expense of neuronal populations. We used immunohistochemical analysis of GFAP expression to label mature astrocytes within the OB. We found a dramatic increase in the number of GFAP positive cells with astrocytic morphology in *Id2*$^{-/-}$ animals localized to the inner granular and germinal layers of the OB suggesting that these cells were emanating from the RMS (Figure 5A, B). This increase is also obvious in aligned coronal sections of the OB from *Id2*$^{-/-}$ and WT mice in a histological pattern suggesting their emergence from the RMS (Figure 5C–F). To extend this observation we used immunohistochemical analysis to examine aligned OB histological sections prepared from mice that had been sacrificed immediately following a 7 day BRDU inoculation regime for GFAP expression and BRDU incorporation (see Experimental Procedures)(B. A. Reynolds and S. Weiss, 1992, 1996). We quantified BRDU single positive and BRDU/GFAP double positive cells within the OB in multiple sections using confocal microscopy (Figure 5G, H). Our finding of decreased BRDU labeled cells within the OB of *Id2*$^{-/-}$ mice (Figure 5G) suggests that fewer cells born in the SVZ and RMS reach the OB of these mice. Also, we found in *Id2*$^{-/-}$ mice a greater percentage of these cells expressed GFAP (Figure 5H) suggesting that either enhanced numbers of neuroblasts differentiate into astrocytes or that fewer neuroblasts fated to differentiate into neurons arrive in the OB. These data support a model in which the loss of *Id2* in RMS neuroblasts contributes to a cell-fate alteration resulting in increased numbers of astroglia and a diminished neuronal cell population in the OB.

Id2 Regulates Growth Kinetics and Differentiation of Cultured Neural Progenitor Cells

Our *in vivo* observations support a model by which a normal SVZ produces appropriate numbers of type-C cells, however, an alteration in cell fate during migration in the RMS leads to an increase in the production of OB astrocytes. An analysis of neural progenitor growth *in vitro* under proliferation conditions following dispersion of neurospheres revealed that *Id2*$^{-/-}$ progenitor cells grew more slowly than cells isolated from WT animals and cultured in an identical manner (Figure 6A). We employed BRDU incorporation quantified by flow cytometry to examine the DNA synthesis at several time points following neurosphere dispersion and plating. We routinely observed that BRDU accumulation was decreased in *Id2*$^{-/-}$ cells compared to WT cells as early as 24 hours following dispersion (Figure 6B). We used DNA content flow cytometry to characterize the cell cycle distribution of neurosphere cultures prepared from WT and *Id2*$^{-/-}$ mice maintained in proliferation conditions. When compared to WT cultures, cultures from *Id2*$^{-/-}$ animals demonstrated a decrease in S-phase cells and a corresponding increase in G_0 cells (G_0: WT 58.57%, *Id2*$^{-/-}$ 73.65%; S-phase: WT 33.37%, *Id2*$^{-/-}$ 21.07%). Consistent with this observation we also observed a decrease in the average neurosphere size attained by *Id2*$^{-/-}$ cells (Figure 6C). To be certain that *Id2*$^{-/-}$ cells *in vitro* were not undergoing increased apoptosis we analyzed the expression of Annexin V in cells cultured in proliferation conditions 24 hours after dispersion. We did not observe any difference between WT and *Id2*$^{-/-}$ cells in the percentage of apoptotic cells that arose under these conditions (data not shown).

To examine the possibility that premature astroglial differentiation within neurospheres growing in proliferation conditions was the cause of decreased cell proliferation and sphere size in *Id2*$^{-/-}$ cultures. For this analysis, neurospheres were dispersed and immediately mounted and fixed on a poly-lysine coated slide at specific time points after the initiation of the cultures. These cells were then immunostained for GFAP. While GFAP expression is a hallmark of rare type-B cells *in vivo*, we did not detect expression at the 24hr time point in WT cells (Figure 6D) and only minimal expression was detected at the 48hr time point indicating that type-B cells would not confound our analysis of astroglial differentiation (Figure 6E). In support of our *in vivo* findings that the OB of *Id2*$^{-/-}$ mice contained an increased number of astroglial cells (Figure 5), cultures from I*d2*$^{-/-}$ mice express GFAP at 24h after plating in proliferation conditions (Figure 6F) and at 48h significantly more GFAP positive cells than were present in cultures from WT animals were observable (Figure 6G). Our finding in these neurosphere cultures of increasing percentages of GFAP positive cells (Figure 6F, G), diminished cellular proliferation, and decreased sphere size suggest that *Id2*$^{-/-}$ cells more avidly undergo astroglial differentiation than do comparable cells from WT animals. We interpret our ability to establish neural progenitor cultures from *Id2*$^{-/-}$ mice as indicating that functional type-B cells must be present. The decreased proliferative rate of these cultures combined with increased numbers of astroglia present under conditions that support proliferation suggests that astroglia from type-C or type-A progeny, which make up the majority of proliferative neurosphere cultures, differentiate during cultivation (B. A. Reynolds and S. Weiss, 1992).

To evaluate the potential mechanisms of cell fate alterations resulting from the loss of *Id2* expression, we explanted neural precursor cells from the SVZ of WT and *Id2*$^{-/-}$ mice and cultured them as neurospheres. Using *in vitro* differentiation techniques (see Experimental Procedures) we induced these cells to differentiate, observed them for 16 days, and used immunochemistry to evaluate the emergence of cells of the neuronal, astrocytic, and oligodendroglial lineages. We observed a multi-layered bed of GFAP positive cells within three days of establishing these cultures and the presence of both oligodendroglial and neuronal lineages by day seven in culture (data not shown). Although a small decrease in the numbers of neuronal cells in *Id2*$^{-/-}$ cultures seemed discernible upon inspection, we were unable to

reliably quantify cells in the various lineages of interest because focal regions with a high percentage of differentiated cells were dispersed within large regions with only very positive rare cells.

Regulation of *Hes1* by *Id2*

Hes1 is a bHLH transcription factor known to be important for the inhibition of neuronal differentiation, although it is permissive of astroglial differentiation (Y. Nakamura et al., 2000; J. Hatakeyama et al., 2004). *Id2* has recently been demonstrated to specifically inhibit *Hes1* auto-repression by directly binding Hes1 protein and preventing it from homo-dimerizing and engaging its own promoter (G. Bai et al., 2007). To determine the effect of Id2 on *Hes1* expression in neural progenitors, we compared the level of *Hes1* transcript in cultured neural progenitor cells from both WT and $Id2^{-/-}$ mice *in vitro* using real-time PCR and found it to be significantly reduced in $Id2^{-/-}$ mice (Figure 7A, D). Also, enhanced expression of Id2 is associated with enhanced expression of Hes1 protein in this cell type (Figure 7B). These findings are consistent with the expectation that loss of Id2 would lead to increased auto-repression and a decreased steady state level of *Hes1* mRNA. We extended this observation to evaluate the effect of Id2 expression in neural progenitors on Hes1 promoter activity. We co-transfected neural progenitors with a luciferase reporter construct that encompasses the entire *Hes1* promoter including the site at which Hes1 binding mediates auto-repression (H. Hirata et al., 2002). Expression from this reporter gene construct in neural progenitors is below detectable levels in the absence of Notch activation (data not shown). We therefore examined the ability of Id2 to alter *Hes1* promoter activity in the presence of N1ICD, an activated form of Notch1, and found that Hes1 promoter activity was greatly enhanced in the presence of Id2 (Figure 7C). These data all support strongly the established notion that Id2 inhibits Hes1 auto-repression (G. Bai et al., 2007), and raises the important possibility that the lack of Id2 in neural progenitors in $Id2^{-/-}$ mice leads to enhanced Hes1 mediated inhibition of its targets, including genes that regulate neural differentiation (G. L. Manglapus et al., 2004).

Ascl1 (Mash1) has been identified as critical to the genesis of dopamineric neurons (C. H. Park et al., 2006), and *Mash1* is a known direct target of Hes1 repression (A. Fischer and M. Gessler, 2007). We therefore examined whether the enhanced transcriptional inhibitory activity of Hes1 in $Id2^{-/-}$ mice affected expression of the pro-neural transcription factor Mash1 in neural progenitor cells. We found reduced expression of Mash1 mRNA in $Id2^{-/-}$ neural progenitor cells using real-time PCR (Figure 7D). This suggests that in the absence of Id2 expression, Hes1 function is enhanced not only as measured by the auto-repression of its own promoter (Figure 7D), but also repression of its endogenous targets. To extend this observation we used short-hairpin RNA (shRNA) stably expressed by retroviral vectors to decrease expression of Hes1 in WT neural precursors cells. We detected increased expression of Mash1 protein in these cells suggesting that endogenous Hes1 expression functions to inhibit transcription of *Mash1* (Figure 7E).

We next sought further evidence of increased Hes1 activity mediating transcriptional inhibition and causing the reduced expression of *Hes1* and *Mash1* (Figure 7D) in $Id2^{-/-}$ cells. Our experiments suggested that loss of *Id2* would result in increased *Hes1* auto-repression as well as increased repression of *Mash1* (Figure 7). We conducted ChIP assays to evaluate the binding of Hes1 to target E-Boxes located within its own promoter (K. Takebayashi et al., 1994), and we detected a robust increase in Hes1 bound this target sequence $Id2^{-/-}$ neural progenitor cells (Figure 7A). This finding provides additional evidence that in $Id2^{-/-}$ cells increased *Hes1* auto-inhibition is responsible for the reduction in *Hes1* transcript (Figure 7A). Next, we examined Hes1 immunoprecipitated chromatin for evidence of increased binding to the *Mash1* promoter. We identified two N-Box target motifs [(−3162 thru-3167) and (−3172 thru −3177) relative to start codon], known target motifs for Hes1 (T. Iso et al., 2003), adjacent to one another in the

5' UTR of the murine *Mash1* genomic sequence. We designed ChIP primers specific for a 225 base-pair fragment encompassing these two target sequences. Using these, we were able to amplify this murine Hes1 target motif within the *Mash1* promoter only in chromatin immunoprecipitated from $Id2^{-/-}$ neural progenitor cultures by anti-Hes-1 antibody (Figure 8B). This indicated that both *Hes1* auto-repression and Hes1 mediated *Mash1* repression were augmented in $Id2^{-/-}$ cells. Based on these observations, we propose an extension of the model developed by Bai *et al*. In our model, *Id2* remains expressed in a subset of migrating neuroblasts, inhibiting Hes1 mediated transcriptional repression as manifested by both decreased *Hes1* auto-repression as well as decreased inhibition of *Mash1* expression. This allows for higher levels of *Mash1* expression in cells expressing *Id2* contributing to the production of dopamergic neurons (C. H. Park et al., 2006). This paradigm indicates a role for *Id2* that is incongruous with its widely known function as an inhibitor of tissue specific differentiation (L. Cai et al., 2000). In this case, *Id2* is required for the differentiation of dopaminergic OB PGL neurons (Figure 2, Figure 8C).

DISCUSSION

Determination of the molecular basis of cell-fate specification and cellular lineage specific maturation during adult neurogenesis is of critical importance for understanding normal nervous system function and may inform future therapeutic strategies for a variety of disorders, especially neurodegenerative disease (D. A. Lim et al., 2007). Using a targeted gene deletion strategy, we have identified a previously unrecognized role for *Id2* in maintaining the size and cellular organization of the OB in adult mice. This is of particular significance because the size of the OB can reflect alterations in the homeostatic mechanisms that balance the death of olfactory neurons throughout life with their replacement by cells originating as multipotent neural progenitor cells in the SVZ. We characterized the decreased size of the OB in $Id2^{-/-}$ mice, and we found a paucity of TH expressing dopaminergic PGL neurons which arose in association with decreased *Mash1* expression, the result of enhanced Hes1 activity in $Id2^{-/-}$ neural precursors. These molecular changes correlate well with our observation of premature glial differentiation, since Hes1, a known inhibitor of neurogenesis (T. Ohtsuka et al., 2006), is permissive of astroglial differentiation (E. Cau et al., 2000).

Although it is possible that these findings reflect changes in early development, many lines of evidence support an unexpected role for *Id2* in adult neurogenesis. The most intriguing of these is the expression pattern of *Id2* in the murine adult brain. While expression of *Id1* and *Id3* is limited in the adult CNS, expression of *Id2* has been observed in adult neural progenitor cells, migrating neuroblasts, and post-mitotic OB PGL interneurons, as well as in the caudate-putamen and substantia nigra (K. Kitajima et al., 2006). This contrasts with the expression pattern of the final mammalian *Id* family member, *Id4*, which is highly expressed in primitive SVZ cells, lower in differentiating neuroblasts, and not present in post-mitotic neurons (Y. Yokota, 2001; K. Yun et al., 2004; K. Kitajima et al., 2006). The expression of *Id2* in adult neural progenitor cells as well as PGL interneurons places it in a small group of transcription factors that are expressed in both primitive neuronal progenitor cells and a subset of their post-mitotic progeny. To date, such transcription factors include Er81 (J. Stenman et al., 2003), Sp8 (R. R. Waclaw et al., 2006), and Pax6 (M. A. Hack et al., 2005; M. Kohwi et al., 2005). Our observations demonstrate a novel and specific pro-neural function for Id2 in the adult CNS. Here, *Id2* is required for the differentiation of a sub-type of olfactory neurons and functions by inhibiting an inhibitor of differentiation, Hes1.

Hes1 is highly expressed in neural stem cells and its expression is associated with the inhibition of pro-neural genes, while down-regulation of *Hes1* is associated with increased expression of pro-neural genes and subsequent differentiation (Y. Nakamura et al., 2000). Hes1 represents an intriguing target for *Id2* in this paradigm due to the ability of Hes1 to positively regulate

neural stem cell and neuroblast proliferation and inhibit neural differentiation, while allowing astrocyte differentiation to occur (Figure 5, Figure 6) (E. Cau et al., 2000; S. J. Morrison et al., 2000; J. Hatakeyama et al., 2004). Id2 has been demonstrated in a number of laboratories to interact directly with Hes1 (A. Jogi et al., 2002; G. Bai et al., 2007). Co-expression of *Id2* with *Hes1* in the RMS may be required for the expression of *Mash1* which initiates dopaminergic differentiation in migrating neuroblasts (S. Saino-Saito et al., 2004). Our data support the hypothesis that Id2 is required to inhibit astrogliogenesis and promote the *Mash1* dependent dopaminergic phenotype by inhibition of Hes1 protein function.

Our studies indicate that while loss of Id2 inhibition of *Hes1* expression in neural progenitor cells *in vitro* greatly decreases cell proliferation, loss of Id2 function *in vivo* does not effect the adult SVZ stem cell population (G. Bai et al., 2007). Rather, loss of Id2 function results in a decrease in the TH expressing dopaminergic subset of newborn neurons in the PGL of the OB. This proneural role for Id2 appears to be highly specific, as loss of *Id2* does not affect CR positive GABAergic OB neurons. Alterations in Notch activation of *Hes1* may be a major factor in this specificity. Notch activation of *Hes1* is currently among the best described repressors of neural differentiation [for review (T. Iso et al., 2003; A. Fischer and M. Gessler, 2007)]. Notch is active in SVZ type-B cells and neuroblasts in the RMS, although this signal is then reduced as cells enter the OB (M. I. Givogri et al., 2006). It appears likely therefore that while Notch activation of *Hes1* is required for maintaining RMS neuroblasts in the undifferentiated state (J. Hatakeyama et al., 2004; G. Bai et al., 2007), attenuation of Notch signaling, as manifested by decreased Hes1 activity, occurs in association with expression of the dopaminergic differentiation program in the RMS (S. Saino-Saito et al., 2004). In support of this model, our data demonstrates that Id2 alters the activity of Hes1 at the post-translational level and is required for dopaminergic cell-fate.

Cellular alterations in the OB of $Id2^{-/-}$ mice share characteristics with the histology of the *small eye* mouse in which *Pax6* is deleted ($Pax6^{-/-}$)(D. Jimenez et al., 2000; M. Kohwi et al., 2005). Also, heterozygous mutations of *PAX6* in humans contribute to CNS malformations which include olfactory dysfunction (A. Malandrini et al., 2001; S. M. Sisodiya et al., 2001). Histological analysis of heterozygous *small eye* adult mice ($Pax6^{+/-}$) reveals that these animals develop an OB, but are deficient in OB PGL dopaminergic neurons (M. Kohwi et al., 2005). It is possible that a pro-dopaminergic role for *Pax6* during development is retained in the adult neurogenic compartment. Our data suggests that *Id2* is critical for TH positive PGL neural differentiation in the adult. We hypothesize that these two transcription factors, Pax6 and Id2, may therefore be active within an as yet undefined pro-dopaminergic signaling program. We have found that Id2 functions in dopaminergic precursors to inhibit Hes1, an inhibitor of differentiation.

In the $Id2^{-/-}$ OB we saw not only a decrease in the number of dopaminergic neurons (Figure 2) but also increased numbers of astroglia (Figure 5). Astrocytic differentiation is often thought of as a default program in such primitive cells as embryonic stem cell derived neural progenitors and adult neural stem cells (F. Doetsch, 2003;T. Nakayama et al., 2006). We provide evidence suggesting that astrogliosis in the $Id2^{-/-}$ mouse (Figure 4,Figure 5) is the result of increased numbers of newborn astrocytes emanating from the RMS (Figure 4,Figure 5). Could Id2 act as a direct inhibitor of an as yet unappreciated bHLH pro-glial cell-fate determinant? Hes1 is known to be permissive of the astroglial cell-fate, while inhibiting neuronal differentiation (J. Hatakeyama et al., 2004). Interestingly, expression of *Hes1* RNA in OB neurons has a pattern strikingly similar to that of *Id2* as identified using *in situ* hybridization [Allen Brain Institute, (www.brain-map.org) (W. Hu et al., 2008)]. Experiments to identify specific signaling programs regulated by Hes1/Id2 interactions should provide insight into the interface of astrocytic and dopaminergic differentiation.

Id2$^{-/-}$ mice do not discriminate different odorants as well as WT mice (Figure 3) presumably as a result of the loss of dopaminergic neurons. Loss of OB dopaminergic neurons and anosmia are characteristics of several neurodegenerative diseases (K. A. Ansari and A. Johnson, 1975;H. W. Berendse et al., 2001;P. J. Moberg et al., 2006;S. M. Kranick and J. E. Duda, 2008). Parkinson's Disease (PD) is associated with alterations in motor function occurring as the result of the degeneration of dopaminergic neurons of the nigrostriatal pathway (R. L. Nussbaum and M. H. Polymeropoulos, 1997), and PD patients are often anosmic. Interestingly, the expression of *Id2* is seen in adult nigrostriatal dopaminergic neurons (K. Kitajima et al., 2006). Alzheimer's disease is associated with altered olfactory capability and depletion of the dopamine transporter (DAT) and the D2 dopamine receptor (J. N. Joyce et al., 1997;J. Djordjevic et al., 2008). Schizophrenia is also associated with anosmia, and is linked to alterations in the function of dopamine receptors (H. Coon et al., 1993;M. Shah et al., 1995;T. Ilani et al., 2001). These observations and the work reported here suggest a role for *Id2* in mediating dopaminergic neural function beyond the OB, and raise the possibility of other more subtle alterations within the brains of mice lacking *Id2*. Currently our laboratory is investigating the potential that other populations of dopaminergic neurons, particularly within the basal ganglia, are affected by the loss of *Id2*. A role for *Id2* in the generation of cerebral dopaminergic neurons would suggest that the *Id2*$^{-/-}$ mouse may be a relevant model for future studies of neurodegenerative disease.

Supplementary Material

Refer to Web version on PubMed Central for supplementary material.

ACKNOWLEDGMENTS

We appreciate greatly the expert assistance of Sarah Purdy Gilman in all animal experiments reported in this manuscript. We thank Dr. Lucy Liaw (Maine Medical Center Research Institute) for N1ICD and Hes1-luciferase constructs. We thank the Laboratories of Drs. Hermes Yeh and Valerie Galton for assistance with histologic and anosmia techniques respectively. We thank Drs. Stephen Lee and Harker Rhodes for ongoing discussions and guidance in the analysis of dopaminergic neurons. For editing this manuscript we thank Tabatha Richardson, for statistical assistance we thank Dr. Jiang Gui, and for technical assistance we thank Eric York and Eve Kemble. This work was supported by funding from the Theodora B. Betz Foundation (MAI) and by a NIH/NINDS Fellowship 1F32NS059126-01A1 (MCH).

REFERENCES

Andres-Barquin PJ, Hernandez MC, Israel MA. Id4 expression induces apoptosis in astrocytic cultures and is down-regulated by activation of the cAMP-dependent signal transduction pathway. Exp Cell Res 1999;247:347–355. [PubMed: 10066362]

Ansari KA, Johnson A. Olfactory function in patients with Parkinson's disease. J Chronic Dis 1975;28:493–497. [PubMed: 1176578]

Bai G, Sheng N, Xie Z, Bian W, Yokota Y, Benezra R, Kageyama R, Guillemot F, Jing N. Id sustains Hes1 expression to inhibit precocious neurogenesis by releasing negative autoregulation of Hes1. Dev Cell 2007;13:283–297. [PubMed: 17681138]

Benezra R, Davis RL, Lockshon D, Turner DL, Weintraub H. The protein Id: a negative regulator of helix-loop-helix DNA binding proteins. Cell 1990;61:49–59. [PubMed: 2156629]

Berendse HW, Booij J, Francot CM, Bergmans PL, Hijman R, Stoof JC, Wolters EC. Subclinical dopaminergic dysfunction in asymptomatic Parkinson's disease patients' relatives with a decreased sense of smell. Ann Neurol 2001;50:34–41. [PubMed: 11456307]

Bertrand N, Castro DS, Guillemot F. Proneural genes and the specification of neural cell types. Nat Rev Neurosci 2002;3:517–530. [PubMed: 12094208]

Bovetti S, Peretto P, Fasolo A, De Marchis S. Spatio-temporal specification of olfactory bulb interneurons. J Mol Histol. 2007

Cai L, Morrow EM, Cepko CL. Misexpression of basic helix-loop-helix genes in the murine cerebral cortex affects cell fate choices and neuronal survival. Development 2000;127:3021–3030. [PubMed: 10862740]

Cau E, Gradwohl G, Casarosa S, Kageyama R, Guillemot F. Hes genes regulate sequential stages of neurogenesis in the olfactory epithelium. Development 2000;127:2323–2332. [PubMed: 10804175]

Chae JH, Stein GH, Lee JE. NeuroD: the predicted and the surprising. Mol Cells 2004;18:271–288. [PubMed: 15650322]

Coon H, Byerley W, Holik J, Hoff M, Myles-Worsley M, Lannfelt L, Sokoloff P, Schwartz JC, Waldo M, Freedman R, et al. Linkage analysis of schizophrenia with five dopamine receptor genes in nine pedigrees. Am J Hum Genet 1993;52:327–334. [PubMed: 8094267]

De Marchis S, Bovetti S, Carletti B, Hsieh YC, Garzotto D, Peretto P, Fasolo A, Puche AC, Rossi F. Generation of distinct types of periglomerular olfactory bulb interneurons during development and in adult mice: implication for intrinsic properties of the subventricular zone progenitor population. J Neurosci 2007;27:657–664. [PubMed: 17234597]

Dellovade TL, Pfaff DW, Schwanzel-Fukuda M. Olfactory bulb development is altered in small-eye (Sey) mice. J Comp Neurol 1998;402:402–418. [PubMed: 9853907]

Djordjevic J, Jones-Gotman M, De Sousa K, Chertkow H. Olfaction in patients with mild cognitive impairment and Alzheimer's disease. Neurobiol Aging 2008;29:693–706. [PubMed: 17207898]

Doetsch F. The glial identity of neural stem cells. Nat Neurosci 2003;6:1127–1134. [PubMed: 14583753]

Doetsch F, Garcia-Verdugo JM, Alvarez-Buylla A. Cellular composition and three-dimensional organization of the subventricular germinal zone in the adult mammalian brain. J Neurosci 1997;17:5046–5061. [PubMed: 9185542]

Doetsch F, Caille I, Lim DA, Garcia-Verdugo JM, Alvarez-Buylla A. Subventricular zone astrocytes are neural stem cells in the adult mammalian brain. Cell 1999;97:703–716. [PubMed: 10380923]

Fischer A, Gessler M. Delta-Notch--and then? Protein interactions and proposed modes of repression by Hes and Hey bHLH factors. Nucleic Acids Res 2007;35:4583–4596. [PubMed: 17586813]

Florio M, Hernandez MC, Yang H, Shu HK, Cleveland JL, Israel MA. Id2 promotes apoptosis by a novel mechanism independent of dimerization to basic helix-loop-helix factors. Mol Cell Biol 1998;18:5435–5444. [PubMed: 9710627]

Galton VA, Wood ET, St Germain EA, Withrow CA, Aldrich G, St Germain GM, Clark AS, St Germain DL. Thyroid Hormone Homeostasis and Action in the Type 2 Deiodinase-Deficient Rodent Brain During Development. Endocrinology. 2007

Garcia-Verdugo JM, Doetsch F, Wichterle H, Lim DA, Alvarez-Buylla A. Architecture and cell types of the adult subventricular zone: in search of the stem cells. J Neurobiol 1998;36:234–248. [PubMed: 9712307]

Gheusi G, Cremer H, McLean H, Chazal G, Vincent JD, Lledo PM. Importance of newly generated neurons in the adult olfactory bulb for odor discrimination. Proc Natl Acad Sci U S A 2000;97:1823–1828. [PubMed: 10677540]

Givogri MI, de Planell M, Galbiati F, Superchi D, Gritti A, Vescovi A, de Vellis J, Bongarzone ER. Notch signaling in astrocytes and neuroblasts of the adult subventricular zone in health and after cortical injury. Dev Neurosci 2006;28:81–91. [PubMed: 16508306]

Guillemot F. Vertebrate bHLH genes and the determination of neuronal fates. Exp Cell Res 1999;253:357–364. [PubMed: 10585258]

Hack MA, Saghatelyan A, de Chevigny A, Pfeifer A, Ashery-Padan R, Lledo PM, Gotz M. Neuronal fate determinants of adult olfactory bulb neurogenesis. Nat Neurosci 2005;8:865–872. [PubMed: 15951811]

Harding JW, Getchell TV, Margolis FL. Denervation of the primary olfactory pathway in mice. V. Long-term effect of intranasal ZnSO4 irrigation on behavior, biochemistry and morphology. Brain research 1978;140:271–285. [PubMed: 626892]

Hatakeyama J, Bessho Y, Katoh K, Ookawara S, Fujioka M, Guillemot F, Kageyama R. Hes genes regulate size, shape and histogenesis of the nervous system by control of the timing of neural stem cell differentiation. Development 2004;131:5539–5550. [PubMed: 15496443]

Hirata H, Yoshiura S, Ohtsuka T, Bessho Y, Harada T, Yoshikawa K, Kageyama R. Oscillatory expression of the bHLH factor Hes1 regulated by a negative feedback loop. Science 2002;298:840–843. [PubMed: 12399594]

Hu W, Saba L, Kechris K, Bhave SV, Hoffman PL, Tabakoff B. Genomic Insights into Acute Alcohol Tolerance. J Pharmacol Exp Ther. 2008

Iavarone A, Garg P, Lasorella A, Hsu J, Israel MA. The helix-loop-helix protein Id-2 enhances cell proliferation and binds to the retinoblastoma protein. Genes Dev 1994;8:1270–1284. [PubMed: 7926730]

Ilani T, Ben-Shachar D, Strous RD, Mazor M, Sheinkman A, Kotler M, Fuchs S. A peripheral marker for schizophrenia: Increased levels of D3 dopamine receptor mRNA in blood lymphocytes. Proc Natl Acad Sci U S A 2001;98:625–628. [PubMed: 11149951]

Iso T, Kedes L, Hamamori Y. HES and HERP families: multiple effectors of the Notch signaling pathway. J Cell Physiol 2003;194:237–255. [PubMed: 12548545]

Jimenez D, Garcia C, de Castro F, Chedotal A, Sotelo C, de Carlos JA, Valverde F, Lopez-Mascaraque L. Evidence for intrinsic development of olfactory structures in Pax-6 mutant mice. J Comp Neurol 2000;428:511–526. [PubMed: 11074448]

Jogi A, Persson P, Grynfeld A, Pahlman S, Axelson H. Modulation of basic helix-loop-helix transcription complex formation by Id proteins during neuronal differentiation. J Biol Chem 2002;277:9118–9126. [PubMed: 11756408]

Joyce JN, Smutzer G, Whitty CJ, Myers A, Bannon MJ. Differential modification of dopamine transporter and tyrosine hydroxylase mRNAs in midbrain of subjects with Parkinson's, Alzheimer's with parkinsonism, and Alzheimer's disease. Mov Disord 1997;12:885–897. [PubMed: 9399211]

Kitajima K, Takahashi R, Yokota Y. Localization of Id2 mRNA in the adult mouse brain. Brain Res 2006;1073–1074:93–102.

Kohwi M, Osumi N, Rubenstein JL, Alvarez-Buylla A. Pax6 is required for making specific subpopulations of granule and periglomerular neurons in the olfactory bulb. J Neurosci 2005;25:6997–7003. [PubMed: 16049175]

Kranick SM, Duda JE. Olfactory dysfunction in Parkinson's disease. Neurosignals 2008;16:35–40. [PubMed: 18097158]

Lemasson M, Saghatelyan A, Olivo-Marin JC, Lledo PM. Neonatal and adult neurogenesis provide two distinct populations of newborn neurons to the mouse olfactory bulb. J Neurosci 2005;25:6816–6825. [PubMed: 16033891]

Lim DA, Huang YC, Alvarez-Buylla A. The adult neural stem cell niche: lessons for future neural cell replacement strategies. Neurosurg Clin N Am 2007;18:81–92. [PubMed: 17244556]ix

Lois C, Garcia-Verdugo JM, Alvarez-Buylla A. Chain migration of neuronal precursors. Science 1996;271:978–981. [PubMed: 8584933]

Malandrini A, Mari F, Palmeri S, Gambelli S, Berti G, Bruttini M, Bardelli AM, Williamson K, van Heyningen V, Renieri A. PAX6 mutation in a family with aniridia, congenital ptosis, and mental retardation. Clin Genet 2001;60:151–154. [PubMed: 11553050]

Manglapus GL, Youngentob SL, Schwob JE. Expression patterns of basic helix-loop-helix transcription factors define subsets of olfactory progenitor cells. J Comp Neurol 2004;479:216–233. [PubMed: 15452857]

Martoncikova M, Racekova E, Orendacova J. The number of proliferating cells in the rostral migratory stream of rat during the first postnatal month. Cell Mol Neurobiol 2006;26:1451–1459.

Merson TD, Dixon MP, Collin C, Rietze RL, Bartlett PF, Thomas T, Voss AK. The transcriptional coactivator Querkopf controls adult neurogenesis. J Neurosci 2006;26:11359–11370. [PubMed: 17079664]

Moberg PJ, Arnold SE, Doty RL, Gur RE, Balderston CC, Roalf DR, Gur RC, Kohler CG, Kanes SJ, Siegel SJ, Turetsky BI. Olfactory functioning in schizophrenia: relationship to clinical, neuropsychological, and volumetric MRI measures. J Clin Exp Neuropsychol 2006;28:1444–1461. [PubMed: 17050269]

Mori K, Shepherd GM. Emerging principles of molecular signal processing by mitral/tufted cells in the olfactory bulb. Semin Cell Biol 1994;5:65–74. [PubMed: 8186397]

Mori S, Nishikawa SI, Yokota Y. Lactation defect in mice lacking the helix-loop-helix inhibitor Id2. Embo J 2000;19:5772–5781. [PubMed: 11060028]

Morrison SJ, Perez SE, Qiao Z, Verdi JM, Hicks C, Weinmaster G, Anderson DJ. Transient Notch activation initiates an irreversible switch from neurogenesis to gliogenesis by neural crest stem cells. Cell 2000;101:499–510. [PubMed: 10850492]

Morshead CM, van der Kooy D. Postmitotic death is the fate of constitutively proliferating cells in the subependymal layer of the adult mouse brain. J Neurosci 1992;12:249–256. [PubMed: 1729437]

Morshead CM, Craig CG, van der Kooy D. In vivo clonal analyses reveal the properties of endogenous neural stem cell proliferation in the adult mammalian forebrain. Development 1998;125:2251–2261. [PubMed: 9584124]

Nakamura Y, Sakakibara S, Miyata T, Ogawa M, Shimazaki T, Weiss S, Kageyama R, Okano H. The bHLH gene hes1 as a repressor of the neuronal commitment of CNS stem cells. J Neurosci 2000;20:283–293. [PubMed: 10627606]

Nakayama T, Sai T, Otsu M, Momoki-Soga T, Inoue N. Astrocytogenesis of embryonic stem-cell-derived neural stem cells: Default differentiation. Neuroreport 2006;17:1519–1523. [PubMed: 16957601]

Nussbaum RL, Polymeropoulos MH. Genetics of Parkinson's disease. Hum Mol Genet 1997;6:1687–1691. [PubMed: 9300660]

Ohtsuka T, Imayoshi I, Shimojo H, Nishi E, Kageyama R, McConnell SK. Visualization of embryonic neural stem cells using Hes promoters in transgenic mice. Mol Cell Neurosci 2006;31:109–122. [PubMed: 16214363]

Park CH, Kang JS, Kim JS, Chung S, Koh JY, Yoon EH, Jo AY, Chang MY, Koh HC, Hwang S, Suh-Kim H, Lee YS, Kim KS, Lee SH. Differential actions of the proneural genes encoding Mash1 and neurogenins in Nurr1-induced dopamine neuron differentiation. J Cell Sci 2006;119:2310–2320. [PubMed: 16723737]

Parrish-Aungst S, Shipley MT, Erdelyi F, Szabo G, Puche AC. Quantitative analysis of neuronal diversity in the mouse olfactory bulb. J Comp Neurol 2007;501:825–836. [PubMed: 17311323]

Petreanu L, Alvarez-Buylla A. Maturation and death of adult-born olfactory bulb granule neurons: role of olfaction. J Neurosci 2002;22:6106–6113. [PubMed: 12122071]

Porteus MH, Bulfone A, Liu JK, Puelles L, Lo LC, Rubenstein JL. DLX-2, MASH-1, and MAP-2 expression and bromodeoxyuridine incorporation define molecularly distinct cell populations in the embryonic mouse forebrain. J Neurosci 1994;14:6370–6383. [PubMed: 7965042]

Reynolds BA, Weiss S. Generation of neurons and astrocytes from isolated cells of the adult mammalian central nervous system. Science 1992;255:1707–1710. [PubMed: 1553558]

Reynolds BA, Weiss S. Clonal and population analyses demonstrate that an EGF-responsive mammalian embryonic CNS precursor is a stem cell. Dev Biol 1996;175:1–13. [PubMed: 8608856]

Saino-Saito S, Sasaki H, Volpe BT, Kobayashi K, Berlin R, Baker H. Differentiation of the dopaminergic phenotype in the olfactory system of neonatal and adult mice. J Comp Neurol 2004;479:389–398. [PubMed: 15514978]

Shah M, Coon H, Holik J, Hoff M, Helmer V, Panos P, Byerley W. Mutation scan of the D1 dopamine receptor gene in 22 cases of bipolar I disorder. Am J Med Genet 1995;60:150–153. [PubMed: 7485250]

Shepherd GM, Chen WR, Willhite D, Migliore M, Greer CA. The olfactory granule cell: from classical enigma to central role in olfactory processing. Brain Res Rev 2007;55:373–382. [PubMed: 17434592]

Shepherd, GMG.; C, A. The Synaptic Organization of the Brain. Vol. 4th Ed.. New York: Oxford University Press; 1998.

Sisodiya SM, Free SL, Williamson KA, Mitchell TN, Willis C, Stevens JM, Kendall BE, Shorvon SD, Hanson IM, Moore AT, van Heyningen V. PAX6 haploinsufficiency causes cerebral malformation and olfactory dysfunction in humans. Nat Genet 2001;28:214–216. [PubMed: 11431688]

Stenman J, Toresson H, Campbell K. Identification of two distinct progenitor populations in the lateral ganglionic eminence: implications for striatal and olfactory bulb neurogenesis. J Neurosci 2003;23:167–174. [PubMed: 12514213]

Stoykova A, Gruss P. Roles of Pax-genes in developing and adult brain as suggested by expression patterns. J Neurosci 1994;14:1395–1412. [PubMed: 8126546]

Takebayashi K, Sasai Y, Sakai Y, Watanabe T, Nakanishi S, Kageyama R. Structure, chromosomal locus, and promoter analysis of the gene encoding the mouse helix-loop-helix factor HES-1. Negative autoregulation through the multiple N box elements. J Biol Chem 1994;269:5150–5156. [PubMed: 7906273]

Waclaw RR, Allen ZJ 2nd, Bell SM, Erdelyi F, Szabo G, Potter SS, Campbell K. The zinc finger transcription factor Sp8 regulates the generation and diversity of olfactory bulb interneurons. Neuron 2006;49:503–516. [PubMed: 16476661]

Yang HK, Sundholm-Peters NL, Goings GE, Walker AS, Hyland K, Szele FG. Distribution of doublecortin expressing cells near the lateral ventricles in the adult mouse brain. J Neurosci Res 2004;76:282–295. [PubMed: 15079857]

Yokota Y. Id and development. Oncogene 2001;20:8290–8298. [PubMed: 11840321]

Yokota Y, Mansouri A, Mori S, Sugawara S, Adachi S, Nishikawa S, Gruss P. Development of peripheral lymphoid organs and natural killer cells depends on the helix-loop-helix inhibitor Id2. Nature 1999;397:702–706. [PubMed: 10067894]

Yun K, Potter S, Rubenstein JL. Gsh2 and Pax6 play complementary roles in dorsoventral patterning of the mammalian telencephalon. Development 2001;128:193–205. [PubMed: 11124115]

Yun K, Mantani A, Garel S, Rubenstein J, Israel MA. Id4 regulates neural progenitor proliferation and differentiation in vivo. Development 2004;131:5441–5448. [PubMed: 15469968]

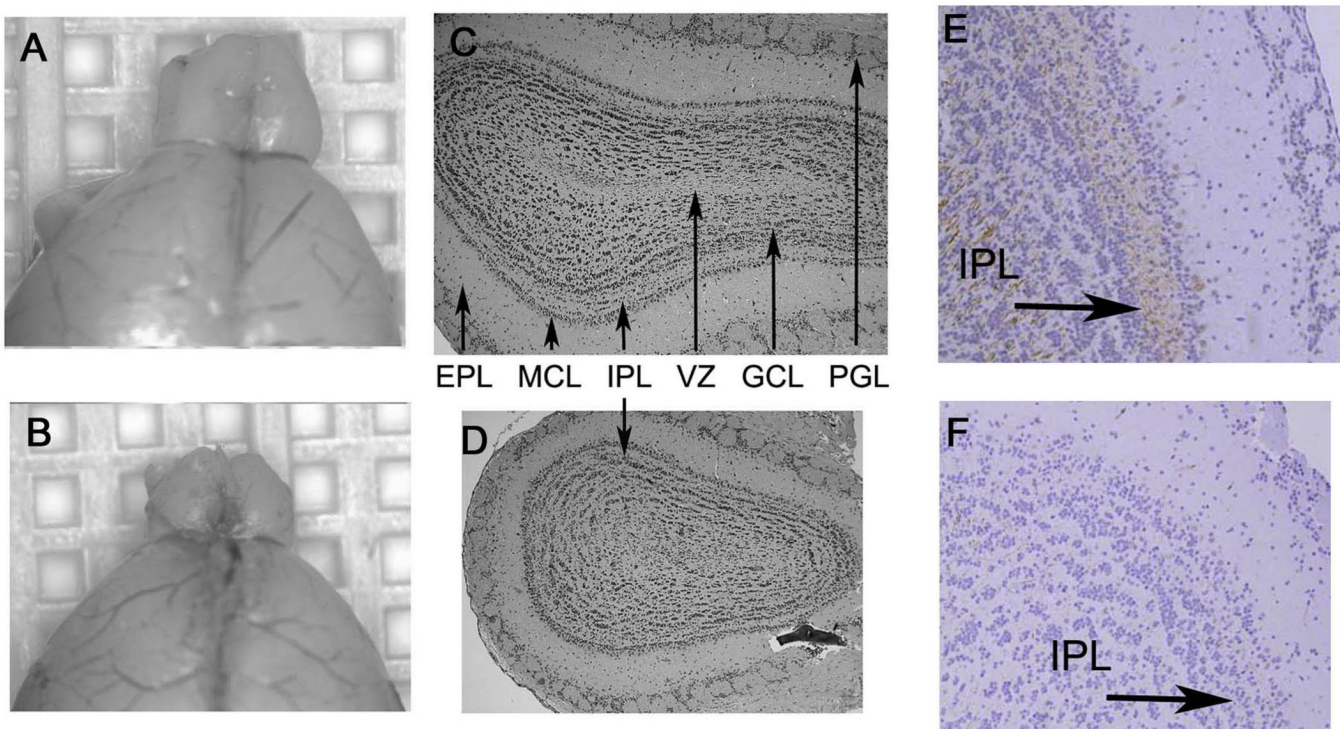

Figure 1. *Id2*$^{-/-}$ Mice Have a Diminished Olfactory Bulb

(A, B) Micrographs of representative gross morphology of WT (A) and *Id2*$^{-/-}$ (B) brains. (C, D) Morphometrically aligned coronal sections stained with hematoxylin and eosin [Periglomerular layer (PGL), external plexiform layer (EPL), mitral cell layer (MCL), internal plexiform layer (IPL), granular cell layer (GCL), and ventricular zone (VZ)]. (E, F) Immunohistochemical evaluation of OB histologic sections from WT (E) and *Id2*$^{-/-}$ (F) mice for neurofilament expression visualized by brown DAB staining and hematoxylin counterstain. Arrows indicate location of IPL, original magnification 40X.

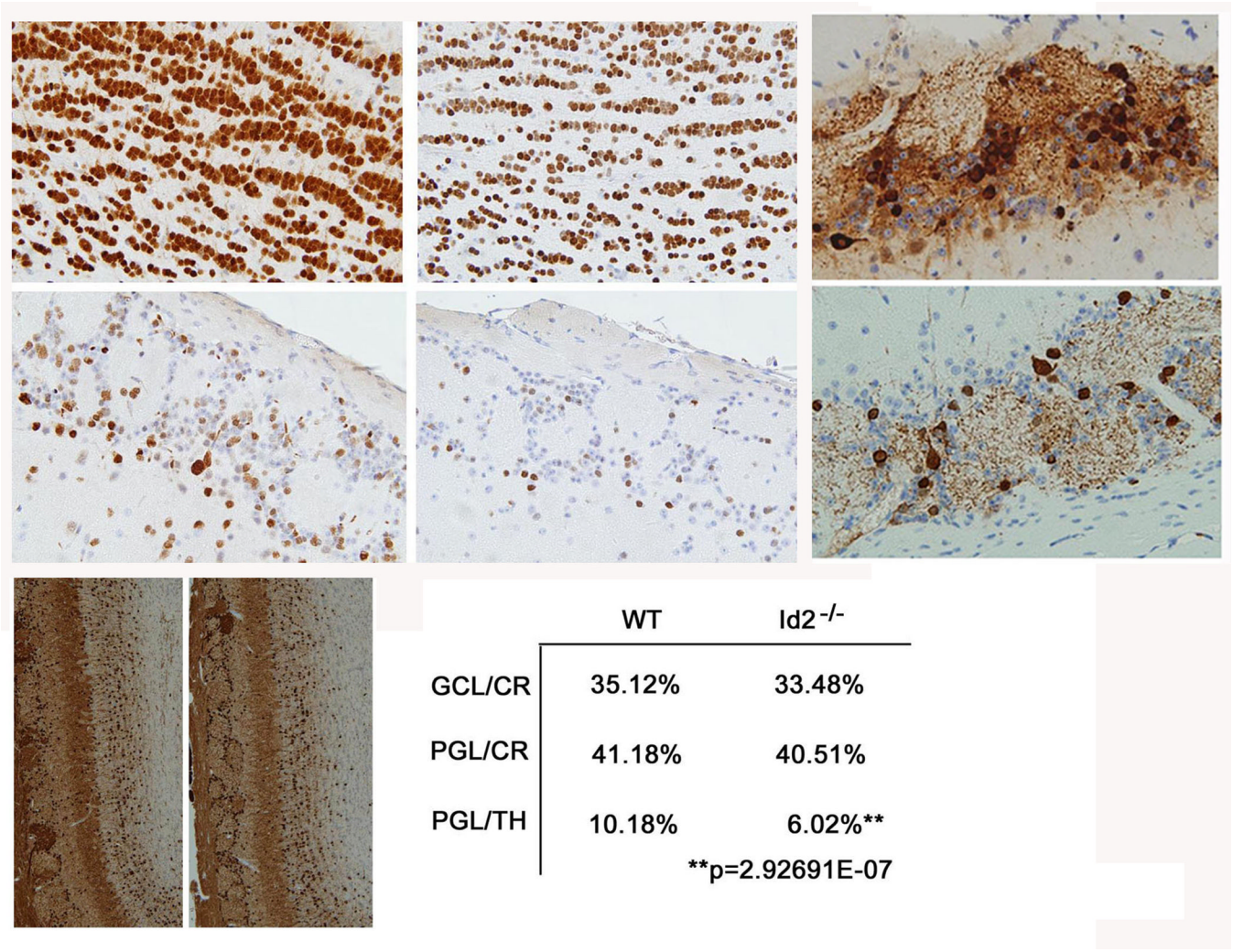

	WT	Id2 -/-
GCL/CR	35.12%	33.48%
PGL/CR	41.18%	40.51%
PGL/TH	10.18%	6.02%**

**p=2.92691E-07

Figure 2. Reduced Olfactory Bulb Size is the Result of Decreased Numbers of Newborn Neurons

Immunohistochemical analysis of total neurons using NeuN anti-sera to evaluate coronal sections of the OB GCL and PGL in WT and *Id2*$^{-/-}$ mice. [(A) -WT GCL, (B) -KO GCL, (C) -WT PGL, (D) -KO PGL, 100 μM^2 areas, 40X magnification n=12)]. (E, F) TH staining of the PGL and GCL in WT (I) and *Id2*$^{-/-}$ (J). (G, H) Coronal sections stained for CR and counterstained with hematoxylin in WT (G) and *Id2*$^{-/-}$ (H) mice. (I) Quantitation of CR and TH expressing cells from serial sections in WT and *Id2*$^{-/-}$ mice (n=3 per group). CR+/GCL p< 0.68, CR+/PGL p< 0.76, TH+/PGL p <4.32E-08, TH+/GCL cells occurred below quantifiable levels.

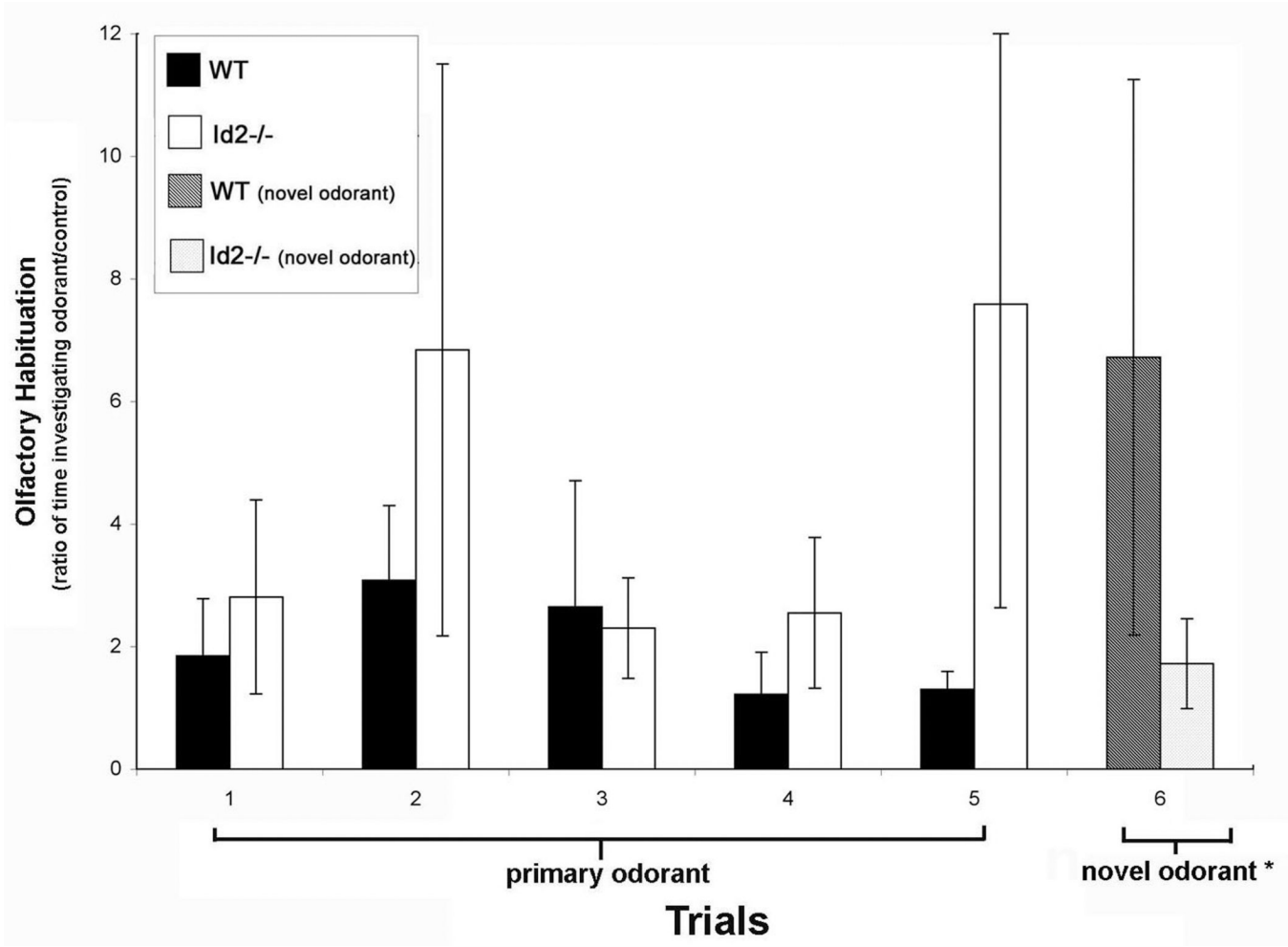

Figure 3. Altered Olfaction in *Id2*$^{-/-}$ Mice

Olfactory discrimination was analyzed using a habituation-dishabituation paradigm (G. Gheusi et al., 2000). To evaluate habituation, mice (n=5 per genotype) were presented with a primary odorant on 5 consecutive trials at 30 minute intervals and the time spent investigating the location of an odorant was designated as a ratio of this duration compared to the time spent investigating a control of unscented water. For the sixth trial a novel odorant was substituted for the primary odorant. The ratios reported represent the average of 2 independent experiments performed in triplicate. Error bars represent SEM. Mann-Whitney-Wilcoxon rank-sum test was performed on the differences between the responses of *WT* and *Id2*$^{-/-}$ mice to the presentation of the novel odorant. W=52, ($p < 0.04$).

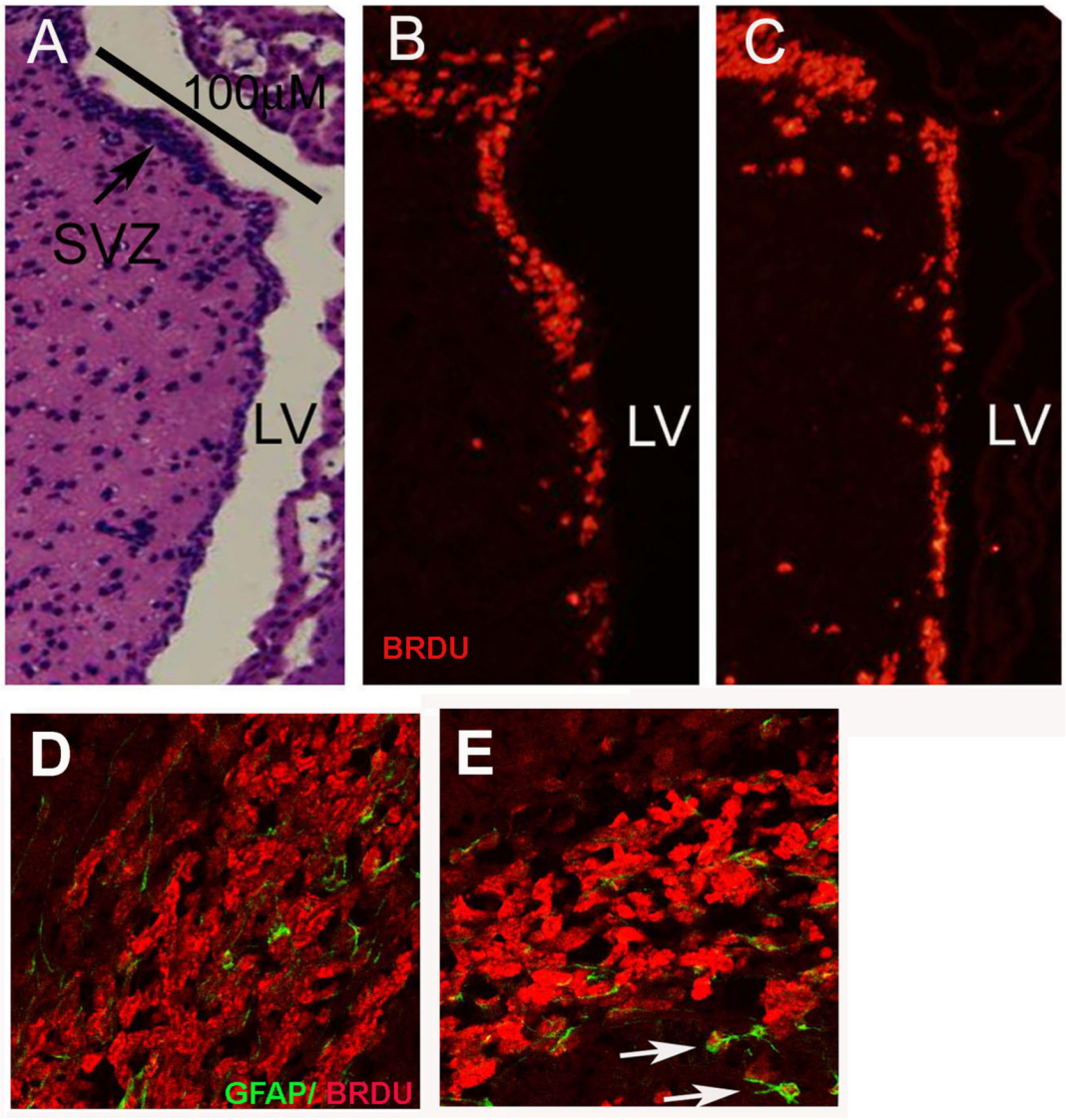

Figure 4. *Id2*$^{-/-}$ Mice Retain Normal Numbers of Neural Progenitor Cells, but the RMS is Reduced in Size and Disorganized

(A–C) Multiple sections taken from short-term BRDU pulsed animals were immunostained to identify BRDU positive cells from a morphometrically matched linear surface along the anterior wall of the SVZ identified in the H&E section by a black bar (A). (B, C) Identification of BRDU positive cells (red) in tissue from *WT* (B) and *Id2*$^{-/-}$ mice (C). (D, E) Confocal images of BRDU/GFAP double-labeling of the RMS in WT (D), and *Id2*$^{-/-}$ (E). (E) Arrows indicate atypical locations for a GFAP/BRDU double-positive cells proximal to the RMS in a representative *Id2*$^{-/-}$ histologic section. In Panels D and E, the red fluorescence corresponds to BRDU incorporation and green fluorescence corresponds to GFAP expression.

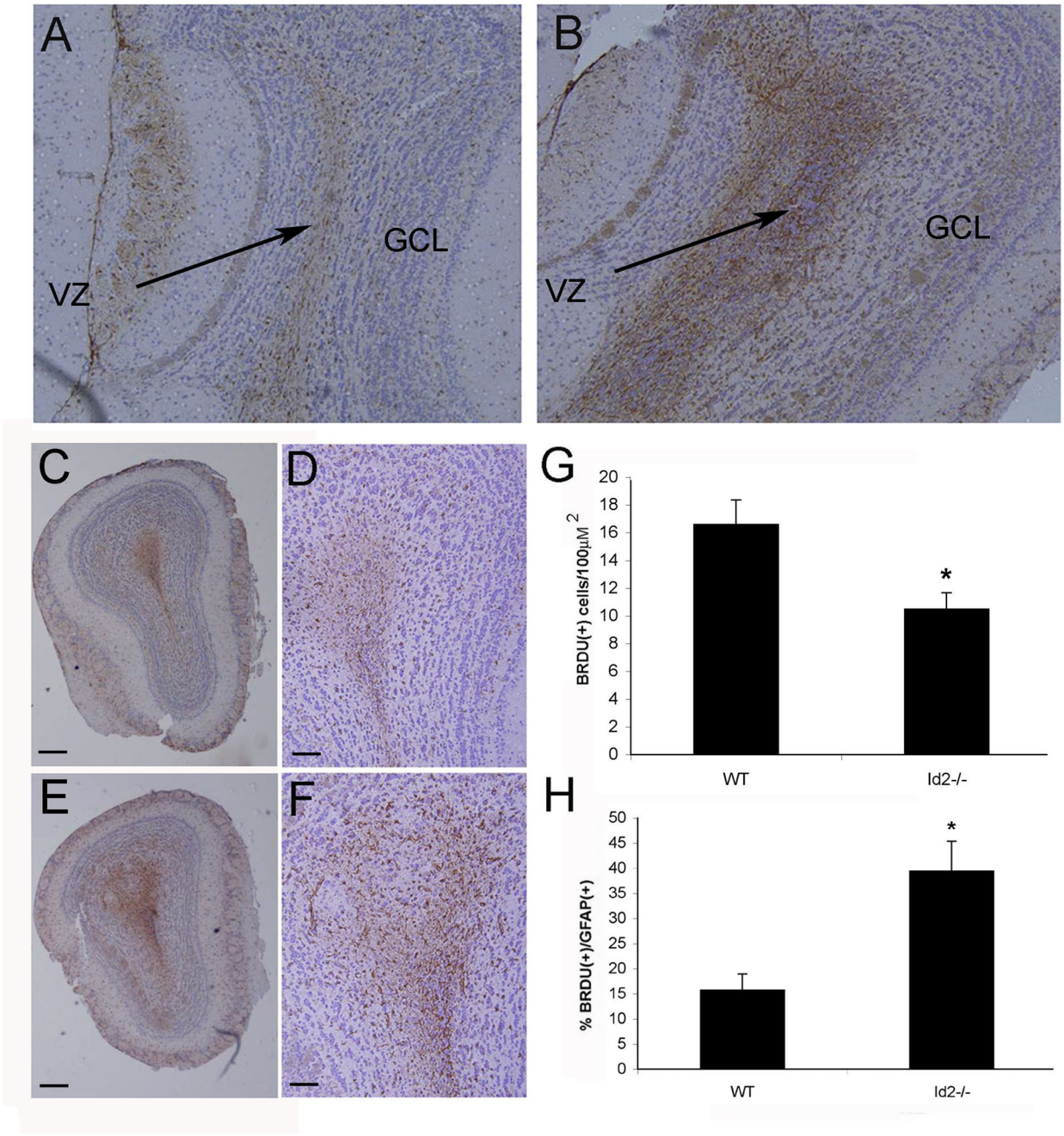

Figure 5. The *Id2*$^{-/-}$ Olfactory Bulb has Increased Numbers of Newborn Astrocytes

GFAP immunohistochemical analysis (brown staining) of saggital (A,B) and coronal (C–F) histologic sections of WT (A, C, D) and *Id2*$^{-/-}$ (B, E, F) OB counterstained with hematoxylin. (A–B) Original magnification 5X. (C, E) Original magnification 5X, C, E scale bars = 100μM, (D, F) Original magnification 20X, D, F scale bars = 50 μM. (G) Using immunofluorescence on frozen sections from animals inoculated for 7 days with BRDU, total BRDU positive cells were quantified in serial confocal micrographs taken from the OB of WT and *Id2*$^{-/-}$ mice. (H) BRDU/GFAP double-labeled newborn astrocytes were quantified in multiple fields (n = 36 fields per genotype) from serial tissue sections and expressed as a percentage of total cells. Error bars represent SEM. (E) $p < 0.023$. (F) $p < 0.005$.

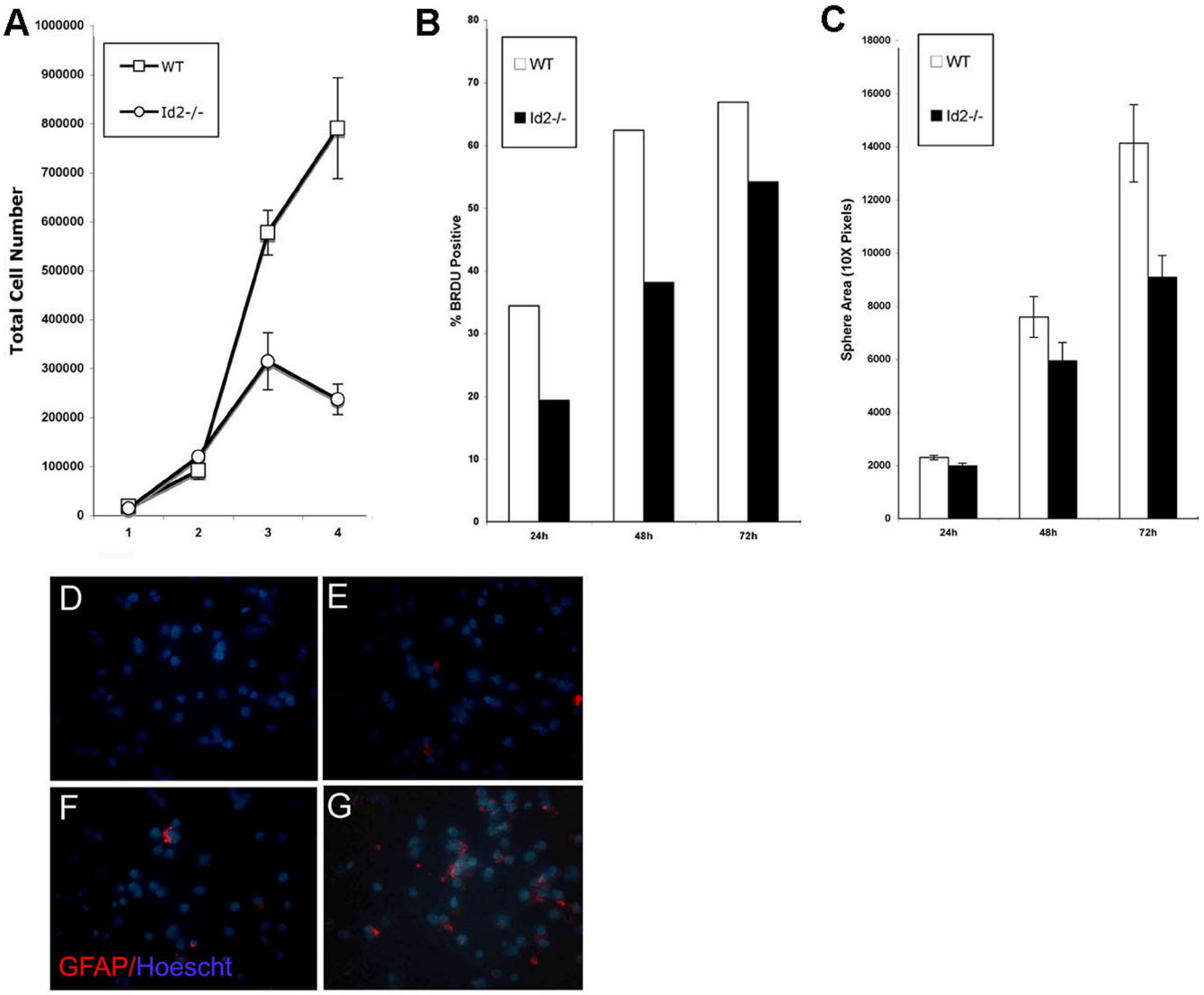

Figure 6. Cultured *Id2*$^{-/-}$ Neural Progenitors Exhibit Altered Growth Kinetics and Premature Astroglial Differentiation

SVZ cells were explanted from neonatal mice and examined for alterations in growth kinetics *in vitro*. (A) Neurospheres were dispersed and cells were plated at an initial density of 20,000 cells in 24 well plates in triplicate and counted days 1 thru 4. (B) BRDU (1mg/ml) was added to neurosphere cultures immediately after dispersion collected at 24, 48, and 72 hours following addition of BRDU. Accumulation of BRDU by WT and *Id2*$^{-/-}$ cells was analyzed using flow cytometry. Results representative of 3 independent experiments are shown. (C) Sphere size was measured using image analysis software 48h after dispersion. (D–G) Neurospheres were dispersed and grown in proliferation conditions for 12 and 24hrs at each time point, cells were dispersed and cytospin cytologic slides of 50,000 cells were immediately prepared. Cytospin preparations were analyzed using GFAP immunofluorescence and Hoescht Dye counterstain [(D) WT, 24h (E) WT, 48h (F) *Id2*$^{-/-}$ (G), 48h].

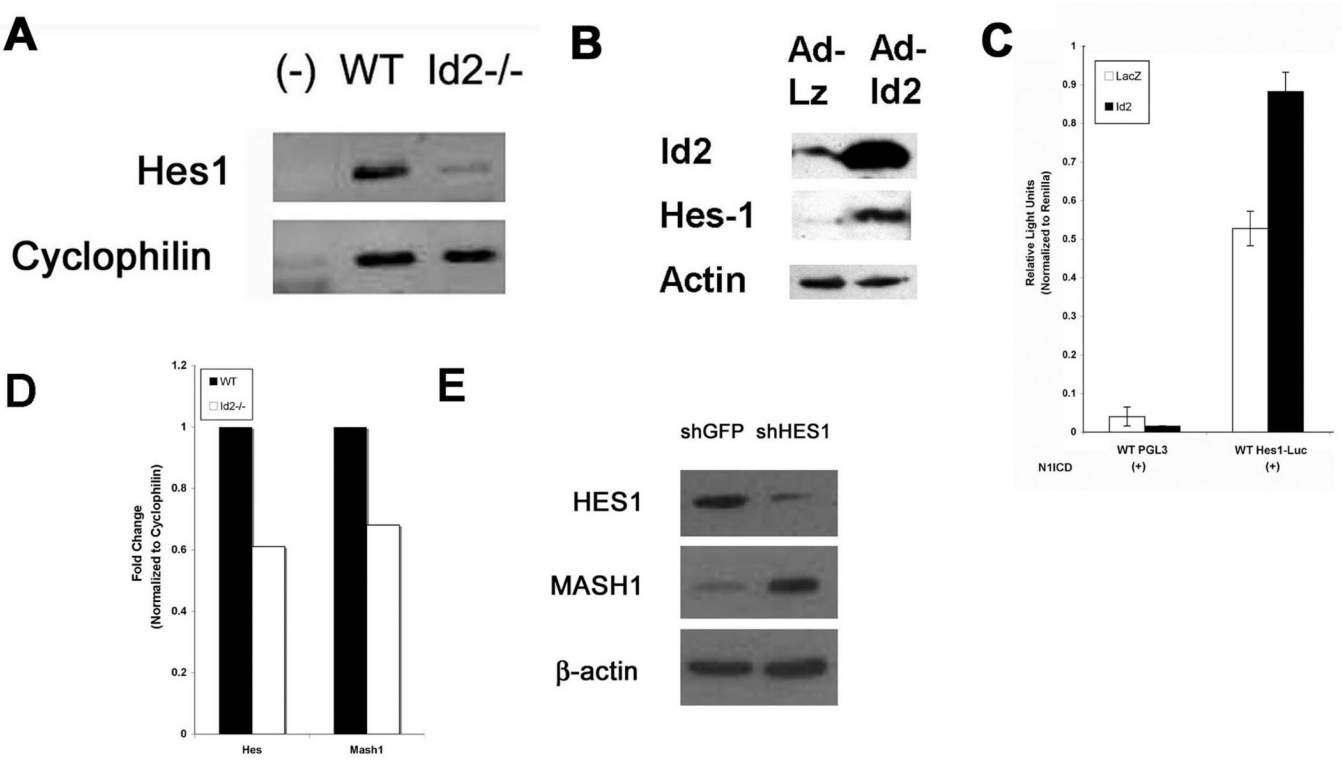

Figure 7. Id2 Regulates the Expression and Activity of Hes1

(A) Total RNA was collected from WT and *Id2*$^{-/-}$ neural progenitor cells, reverse transcribed, and analyzed for *Hes1* mRNA using RT-PCR. (B) Western blot indicating that transient expression of Id2 using adenovirus results in increased expression of Hes1 protein. (C) Luciferase reporter assays were conducted using firefly luciferase driven by the Hes1 promoter. Hes1 reporter activity was induced by co-transfection with constitutively activated Notch1. Addition of Id2 adenovirus resulted in increased activity of the reporter as compared to the LacZ control virus. (D) A representative experiment of Real-Time PCR analysis of *Hes1* and *Mash1* mRNA levels in cultured neural progenitor cells, from WT and *Id2*$^{-/-}$ mice. (E) Stable cell lines were created by infections with retroviral vectors expressing shRNA directed against the Hes1 or a control virus expressing shRNA directed against eGFP in cultured neural progenitor cells. Western blot indicates that Hes1 knock-down results in increased expression of Mash1.

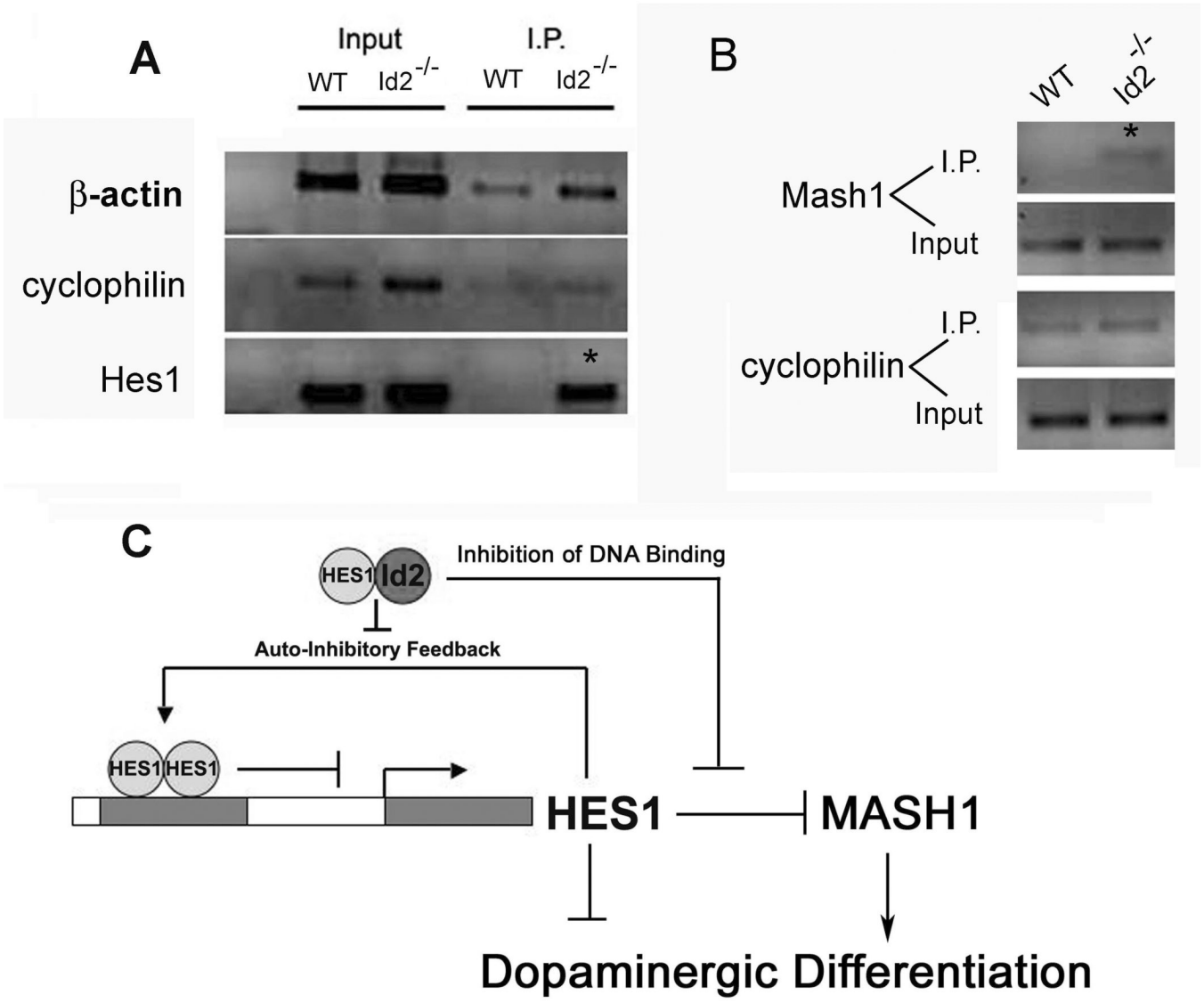

Figure 8. Loss of *Id2* results in direct Hes1 mediated repression of *Hes1* and *Mash1* promoters

Chromatin Immunoprecipitation (ChIP) was conducted in order to determine whether the loss of *Id2* resulted in increased Hes1 function. (A) PCR analysis of a known *Hes1* auto-regulatory domain was conducted following pre-clearing and ChIP with Hes1 anti-sera in WT and *Id2*$^{-/-}$ neurospheres. (B) Further analysis of Hes1 immunoprecipitated DNA fragments using primers directed at a putative Hes1 binding site within the *Mash1* promoter. In all ChIP experiments specificity was demonstrated in all trials by amplification of the housekeeping genes β-actin and cyclophilin in addition to target genes in both input and post-IP material. (C) A novel model of Id2 function by which Id2 blocks the auto-repression of *Hes1*. Loss of Id2 results in both increased Hes1 auto-repressive function as well as inhibiting the expression of *Mash1*, a gene important in a pro-dopaminergic cell-fate program required during adult neurogenesis.